Comments on Inorganic Chemistry
Publication details, including instructions for authors and subscription information:
http://www.informaworld.com/smpp/title~content=t713455155

Magnetic Field Effects on the Luminescence of Transition Metal Complexes

Günter Gliemann[a]
[a] Institut für Physikalische und Theoretische Chemie, Universität Regensburg, Federal Republic of Germany

To cite this Article Gliemann, Günter(1986) 'Magnetic Field Effects on the Luminescence of Transition Metal Complexes', Comments on Inorganic Chemistry, 5: 6, 263 — 284
To link to this Article: DOI: 10.1080/02603598608081848
URL: http://dx.doi.org/10.1080/02603598608081848

Magnetic Field Effects on the Luminescence of Transition Metal Complexes

In many crystalline transition metal complexes the radiative deactivation of the lowest excited electronic state is only vibronically allowed. By application of an external magnetic field the deactivation process can become directly allowed without assistance of a vibrational quantum and, thus, the luminescence is blue shifted by the order of one vibrational quantum. Required for this effect is a magnetic-field-induced coupling between the lowest excited electronic state and a second, energetically adjacent excited electronic state of proper symmetry. Several d^8- and d^6-complex ions are discussed as examples.

INTRODUCTION

There is increasing interest in the nature of the excited electronic states of transition metal complexes for several reasons. As an important example, aspects of photochemistry,[1] where the properties of the low-lying excited states determine the chemical reactions which follow the optical excitation, may be cited.

Appropriate methods for the investigation of these states are the various kinds of spectroscopy, especially optical absorption and emission spectroscopy, since the excited electronic states are directly involved in the corresponding spectra. If the complexes form single crystals, additional information regarding the excited states can be obtained by the application of polarized spectroscopy.[2] In this case the spectra yield much more than the transition energies. The polarization dependence of the transitions reflects the symmetry of the excited states.[3]

Comments Inorg. Chem.
1986, Vol. 5, No. 6, pp. 263–284
0260-3594/86/0506-0263/$25.00/0

By application of external fields, the absorption and emission properties of crystalline transition metal complexes can be influenced positively. Besides investigations at high pressure[4] the effect of homogeneous magnetic fields **H** on the polarized emission has proved to be very informative. In experiments of that kind the relative orientations of the crystal axes (molecular axes), of the electric field vector **E** of the emitted light, of the magnetic field vector **H**, and of the direction **O** of observation can be varied. Since the optical transition probability depends both on the symmetry of the states involved and on the relative orientations mentioned above, the symmetry of the states can be inferred from the polarization properties of the spectra.

EXPERIMENTAL TECHNIQUE

The scheme of a typical apparatus for polarized fluorescence spectroscopy in the presence of external magnetic fields is shown in Fig. 1. The sample (S), a single crystal, is mounted within the liquid helium bath cryostat of a superconducting magnet system (SM). Magnetic field strengths up to several T (Tesla) are required. The excitation source for the CW spectra is, for example, a laser (L). The polarization of the emitted light can be determined by appropriate orientation of the polarizer (P). To avoid falsifying

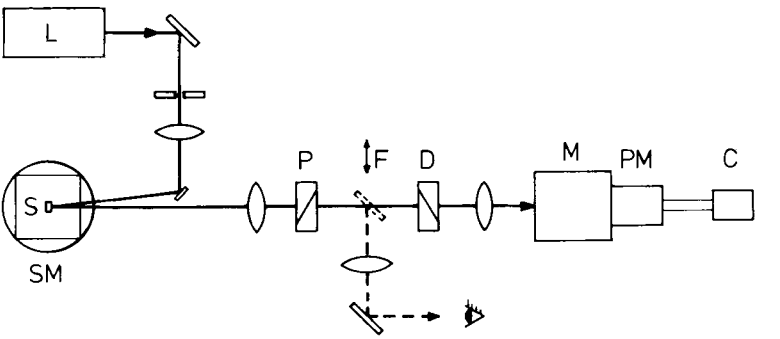

FIGURE 1 Schematic diagram of the apparatus for polarized fluorescence spectroscopy with external magnetic fields. L: Laser, S: sample, SM: superconducting magnet system, P: polarizer, F: movable mirror, D: depolarizer, M: monochromator, PM: photomultiplier, C: microprocessor.

polarization effects by the monochromator (M), the emitted light has to be depolarized by the depolarizer (D) before entering the monochromator. A cooled photomultiplier (PM) detects the emitted light, and the resulting signals can be processed by a microprocessor (C). For time-resolved fluorescence spectroscopy a synchronously pumped laser system consisting of a mode-locked ion laser and a cavity-dumped dye laser can be used as the pulsed excitation source.[5,6]

A very helpful device is the addition of a microscope ocular which extends the spectroscope to a polarization microscope. By shifting the mirror (F) into the beam, exactly that part of the sample which emits the luminescence can be observed visually as is done in polarization microscopy. Thus the final adjustment of the orientation of the single crystal sample can be controlled.

Figure 2 shows the relative directions of the oriented quantities involved in the experiment: the electric field vectors $\mathbf{E}_{exit}$ and $\mathbf{E}$ of the exciting and the emitted light, respectively, the external

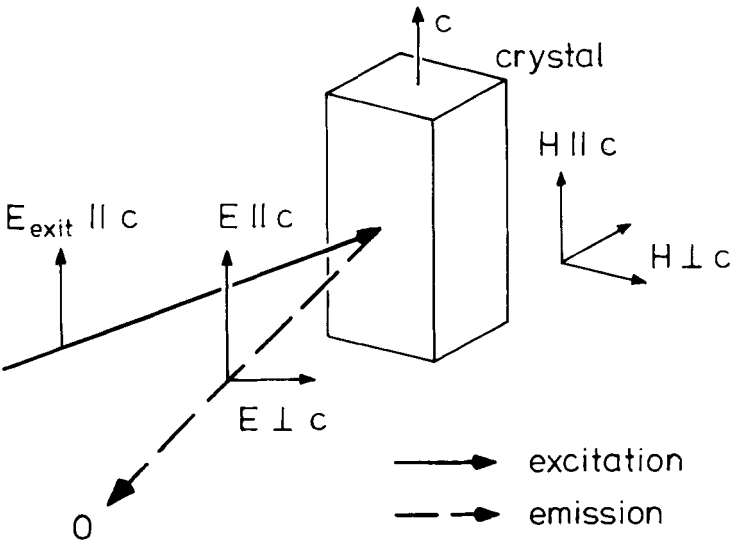

FIGURE 2 Relative directions of the vector quantities. $\mathbf{E}_{exit}$ and $\mathbf{E}$: electric field vectors of the exciting and the emitted radiation, respectively. $\mathbf{H}$: vector of the external homogeneous magnetic field. $\mathbf{O}$: direction of observation. $\mathbf{c}$: direction of the crystallographic c axis.

homogeneous magnetic field **H**, the direction of observation **O**, and the **c** axis of the single crystal. The measurements are preferably performed by backward scattering.

THEORY

Figure 3 shows the low-energy part of the electronic level diagram of a transition metal complex. It is composed of the ground-state level 0 and the three lowest excited electronic levels 1, 2, 3 with energies E_0, E_1, E_2, E_3, respectively. If the electronic state i is described by the wave function $|i\rangle$, then the probability of an electric dipole transition between the states i and j is proportional to the square of the matrix element $\langle i|\mathbf{D}|j\rangle$ where **D** is the electric dipole moment operator.[3] The matrix element vanishes when the product of the representations $\Gamma(i)$, $\Gamma(\mathbf{D})$, and $\Gamma(j)$ does not contain the totally symmetric representation Γ_{tot} of the symmetry group of the complex. In systems with $\Gamma(0) = \Gamma_{tot}$ the electric dipole transitions between the ground state and all excited states i which transform as **D**, $\Gamma(i) = \Gamma(\mathbf{D})$, are allowed. In Fig. 3 this case is assumed with $i = 1, 2, 3$. Thus, emission frequencies ω_1 and ω_2 are expected, with intensities depending on the values of the matrix elements $\langle 1|\mathbf{D}|0\rangle$ and $\langle 2|\mathbf{D}|0\rangle$, respectively.

Vibronic Coupling

In the diagram on the left-hand side of Fig. 4 the electric dipole transition $1 \rightarrow 0$ is assumed to be forbidden. Then a radiative deactivation of the vibrationally nonexcited state 1 can result only by transfer to a vibrationally excited ground state 0 with transition frequency $\omega_1 - \omega_{vib}$. The probability of such a *vibronic* transition is small compared with the probability of an electric-dipole-allowed transition, as can be seen from the mechanism of vibronic transitions.[7,8]

The Hamiltonian $\hat{H}$ describing the electronic states depends on the electron coordinates $\mathbf{r}_{el}$ and, parametrically, on the positions of the nuclei. $\hat{H}$ can be written as a function of the normal coordinates $Q_1, \ldots, Q_f$ of the system, $\hat{H} = \hat{H}(\mathbf{r}_{el}; Q_1, \ldots, Q_f)$. For small displacements of the nuclei from their equilibrium positions

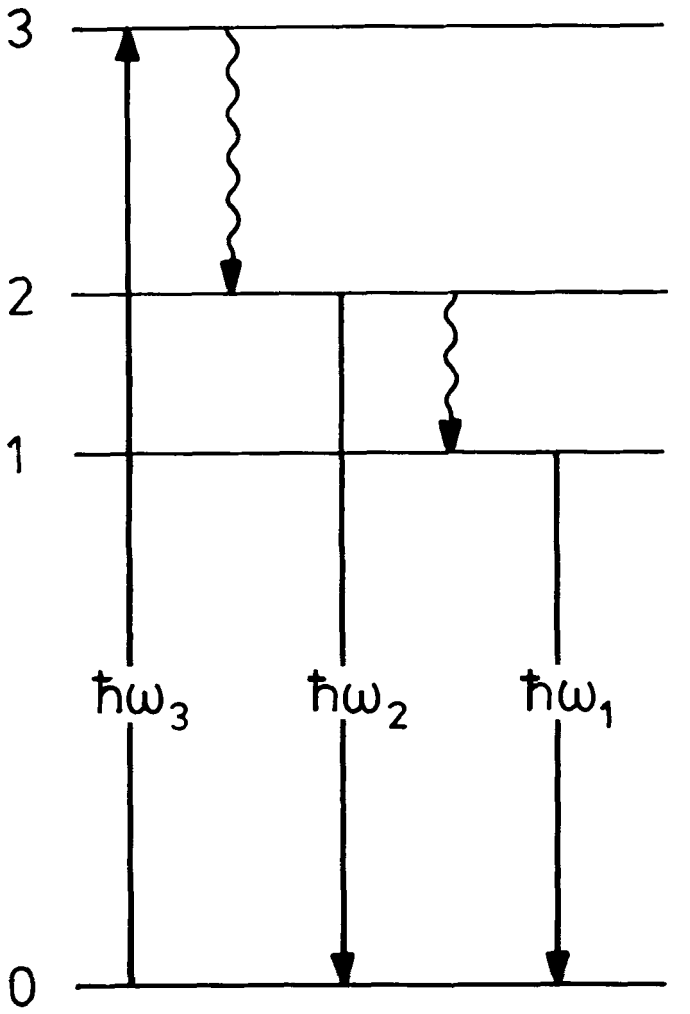

FIGURE 3 Low-energy part of the electronic level diagram of a transition metal complex. →: radiative transitions; ⇝: nonradiative transitions. All transitions between the ground state 0 and the excited states 1, 2, 3 are assumed to be electric-dipole-allowed. $\hbar\omega_i = E_i - E_0$.

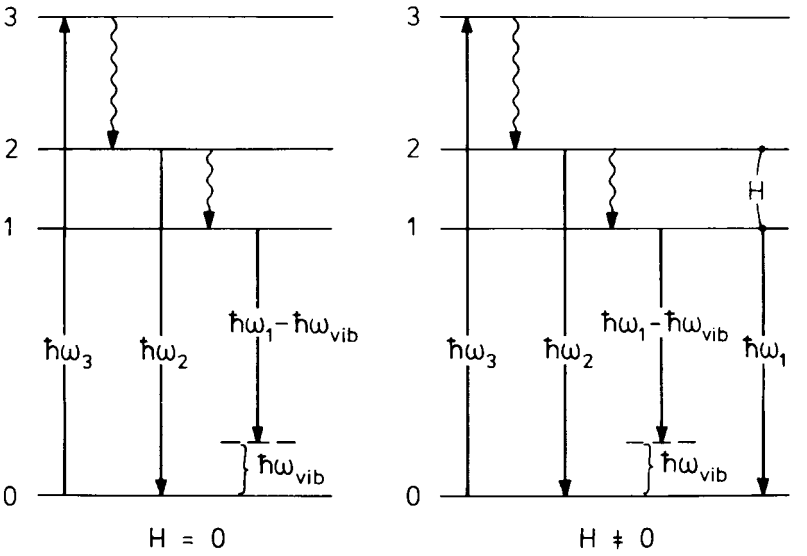

FIGURE 4 Low-energy part of the electronic level diagram of a transition metal complex. →: radiative transitions; ⇝: nonradiative transitions. Left-hand side: Zero-field case ($H = 0$). The transitions between the excited states 2, 3 and the ground state 0 are assumed to be electric-dipole-allowed with transition energies $\hbar\omega_{2,3} = E_{2,3} - E_0$. The transition $1 \rightarrow 0$ is vibronically allowed with energy $\hbar\omega_1 - \hbar\omega_{vib} = [E_1 - E_0] - \hbar\omega_{vib}$. Right-hand side: A magnetic field **H** couples the electronic states 1 and 2 and induces the additional direct transition $1 \rightarrow 0$ with energy $\hbar\omega_1 = E_1 - E_0$. The relatively small Zeeman shifts of the levels are omitted.

$Q_n = 0, n = 1, \ldots, f$, the following expansion at $Q_n = 0$ holds:

$$\hat{H}(\mathbf{r}_{el}; Q_1, \ldots, Q_f) = \hat{H}(\mathbf{r}_{el}; 0, \ldots, 0) + \sum_{n=1}^{f} \left(\frac{\partial \hat{H}}{\partial Q_n}\right)_0 \cdot Q_n. \qquad (1)$$

In order that $\hat{H}$ transform according to the totally symmetric representation Γ_{tot} of the symmetry group, each derivative $(\partial \hat{H}/\partial Q_n)_0$ in this expansion must have the same symmetry transformation properties as the corresponding normal coordinate Q_n. As a consequence of the Q dependence of the Hamiltonian, the electron motion couples with the nuclear motion and a mixing of different

electronic states results (*vibronic coupling*). First-order perturbation theory yields electronic wave functions of the type

$$|i\rangle = |i\rangle_0 + \sum_{\lambda \neq i} \frac{\sum_{n=1}^{f} Q_n \langle \lambda | (\partial \hat{H}/\partial Q_n)_0 | i \rangle_0}{E_i - E_\lambda} |\lambda\rangle_0 \qquad (2)$$

where $|i\rangle_0$ and $|\lambda\rangle_0$ are the electronic wave functions derived for the equilibrium positions of the nuclei, and E_i and E_λ are the corresponding energies. Therefore, $|\lambda\rangle_0$ can be mixed with $|i\rangle_0$ only if the system has a normal coordinate Q_n of appropriate symmetry, so that $\Gamma(i) \times \Gamma(Q_n) \times \Gamma(\lambda) \supset \Gamma_{tot}$. Because of the denominator in the mixing coefficients, the degree of admixture will be significant only for pairs of states whose energy separations are not too large.

In the frame of the Born–Oppenheimer approximation, the vibronic states can be described by the product of the electronic wave function $|i\rangle$ and the vibrational function $\chi_{v_1}(Q_1) \cdot \chi_{v_2} \cdot (Q_2) \cdot \cdot \cdot \chi_{v_f}(Q_f)$:

$$\Psi(i; v_1, \ldots, v_f) = |i\rangle \cdot \prod_{n=1}^{f} \chi_{v_n}(Q_n). \qquad (3)$$

The $\chi_v(Q)$ can be approximated by harmonic oscillator wave functions.

For a system in its vibrational ground state ($v_n = 0$ for all n) and in an electronic state $|i\rangle$, which contains an admixture of another electronic state $|s\rangle_0$, the total state function has the following form:

$$\Psi(i;0, \ldots, 0) = |i\rangle_0 \cdot \prod_{n=1}^{f} \chi_0(Q_n) + c_{is,\sigma} \cdot |s\rangle_0 \cdot \chi_1(Q_\sigma) \prod_{\substack{n=1 \\ n \neq \sigma}}^{f} \chi_0(Q_n) \qquad (4)$$

where $c_{is,\sigma} = \langle s | (\partial \hat{H}/\partial Q_\sigma)_0 | i \rangle_0 \, [\sqrt{2}\,(E_i - E_s)]^{-1}$ is the mixing coefficient of the electronic wave functions and Q_σ is the normal co-

ordinate with the appropriate symmetry allowing mixing with $|s\rangle_0$. In Eq. (4) use is made of the general relation for harmonic oscillator wave functions, $Q_n \cdot \chi_0(Q_n) = \chi_1(Q_n)/\sqrt{2}$.

If $|j\rangle$ represents a further electronic state of the system with the matrix elements $\langle j|\mathbf{D}|i\rangle_0 = 0$ and $\langle j|\mathbf{D}|s\rangle_0 \neq 0$, the electric dipole transition between $|i\rangle$ and $|j\rangle$ is "vibronically" allowed because $|i\rangle$ contains a vibronically induced $|s\rangle_0$ admixture. The corresponding transition integral with the total state functions $\Psi(i;0, \ldots ,0)$ and $\Psi(j;v_1, \ldots ,v_f)$ will yield a nonvanishing value only if the final state $|j\rangle$ is excited in the normal vibrational mode Q_σ. Since the coefficient $c_{is,\sigma}$ usually is small compared to unity, the probabilities of such vibronic transitions are much weaker than the directly allowed processes.

The left-hand side of Fig. 4 shows an example of vibronic coupling. By mixing of state 2 ($=|s\rangle_0$) with state 1 ($=|i\rangle_0$), a radiative transition from state 1 to the vibrationally excited ground state 0 ($=|j\rangle$) becomes vibronically allowed with $\omega_{vib} = \omega(Q_\sigma)$.

Magnetic Coupling

When a molecular system in the electronic state $|i\rangle$ is exposed to an external magnetic field $\mathbf{H}$, the magnetic moment $\mathbf{M}_i$ of the electronic system will interact with the magnetic field, yielding a paramagnetic excess energy (Zeeman energy) Δ_i, which is proportional to the magnetic field strength $|\mathbf{H}| = H$:

$$\Delta_i = \mathbf{M}_i \cdot \mathbf{H} \sim H.$$

Since the magnetic interaction is a small perturbation, its energy Δ_i can be calculated by first-order perturbation theory. The perturbation operator $\hat{H}_{mag}$ represents the interaction energy $\mathbf{M}_i \cdot \mathbf{H}$. For a nondegenerate state it results in the following "Zeeman shift":

$$\Delta_i = \langle i|\hat{H}_{mag}|i\rangle = K_i \cdot H$$

where K_i is a constant depending only on the orientation, but not on the absolute value of $\mathbf{H}$. In the case of degeneracy, Δ_i is calculated from the corresponding secular determinant.

For a d-orbital in a transition metal complex exposed to a mag-

netic field strength of $H \approx 1\ \mathrm{T} = 10000$ Gauss, the Zeeman shift is of the order of 10 cm^{-1}. This shift is more than one order of magnitude *smaller* than the magnetic-field-induced energy shift of the luminescence observed with several transition metal complexes, as will be shown below. The effects of the Zeeman shift are not further discussed in this Comment.

There is, however, another magnetic field effect which can strongly influence the luminescence behavior.[5,9] According to perturbation theory the ith electronic state perturbed by a magnetic field **H** can be described by the wave function

$$|i\rangle_H = |i\rangle + \sum_{\mu \neq i} \frac{\langle \mu|\hat{H}_{\mathrm{mag}}|i\rangle}{E_i - E_\mu}|\mu\rangle = |i\rangle + H \cdot \sum_{\mu \neq i} \rho_{\mu i} \cdot |\mu\rangle$$

with

$$\rho_{\mu i} = \frac{1}{H} \cdot \frac{\langle \mu|\hat{H}_{\mathrm{mag}}|i\rangle}{E_i - E_\mu}.$$

Thus, because of $\hat{H}_{\mathrm{mag}} \sim H$, the admixture of a function $|\mu\rangle$ to $|i\rangle$ is proportional to the magnetic field strength H, provided that the coupling integral $\langle \mu|\hat{H}_{\mathrm{mag}}|i\rangle$ does not vanish.

This magnetic field dependence of the state functions can drastically influence radiative deactivation processes. As an important example the right-hand side of Fig. 4 shows a four-level system of states $|0\rangle$, $|1\rangle$, $|2\rangle$, and $|3\rangle$. To reveal the core of the matter we make the following two assumptions:

First, there is practically no magnetic-field-induced admixture of excited states with the electronic ground state: $|0\rangle_H = |0\rangle$. This assumption is justified by the fact that in most transition metal complexes the excited electronic states are located energetically far above the ground state. Second, the state $|1\rangle$ mixes with only *one* of the excited states, the state $|2\rangle$:

$$|1\rangle_H = |1\rangle + H \cdot \rho_{21} \cdot |2\rangle.$$

This assumption is only for convenience and could be dropped without difficulty.

The magnetic field effects are particularly conspicuous for the

luminescence behavior in cases where, in the absence of a magnetic field, the transition $2 \rightarrow 0$ is electric-dipole-allowed, whereas $1 \rightarrow 0$ is electric-dipole-forbidden (but vibronically allowed):

$$\langle 0|\mathbf{D}|2\rangle \neq 0, \quad \langle 0|\mathbf{D}|1\rangle = 0.$$

If the states $|2\rangle$ and $|1\rangle$ mix under the influence of the magnetic field, then we have the transition integrals

$$\langle 0|\mathbf{D}|2\rangle_H = \langle 0|\mathbf{D}|2\rangle \neq 0,$$

$$\langle 0|\mathbf{D}|1\rangle_H = H \cdot \rho_{21} \cdot \langle 0|\mathbf{D}|2\rangle \sim H,$$

which entails the following three results. First, in addition to the electric dipole transition $2 \rightarrow 0$ (frequency ω_2) and the vibronic transition $1 \rightarrow 0$ (frequency $\omega_1 - \omega_{vib}$), a new radiative channel $1 \rightarrow 0$ with frequency ω_1 appears. Second, since the intensity I of an optical emission is proportional to the square of the transition moment, the intensity $I_{1\rightarrow 0}$ of the new transition $1 \rightarrow 0$ is proportional to H^2:

$$I_{1\rightarrow 0} \sim |\langle 0|\mathbf{D}|1\rangle_H|^2 \sim H^2.$$

Third, the rate of a radiative deactivation is likewise proportional to the square of the transition moment:

$$\frac{1}{\tau^r\,(1 \rightarrow 0)} \sim |\langle 0|\mathbf{D}|1\rangle_H|^2 \sim H^2.$$

The consequences of these theoretical results will be demonstrated for typical examples in the next section.

APPLICATIONS

Tungsten(0) Carbonyls

As an example, Fig. 5 shows the structure of the pentacarbonylpyridinetungsten(0) molecule. The intramolecular z axis is defined as the direction of the metal–nitrogen bond. The crystal

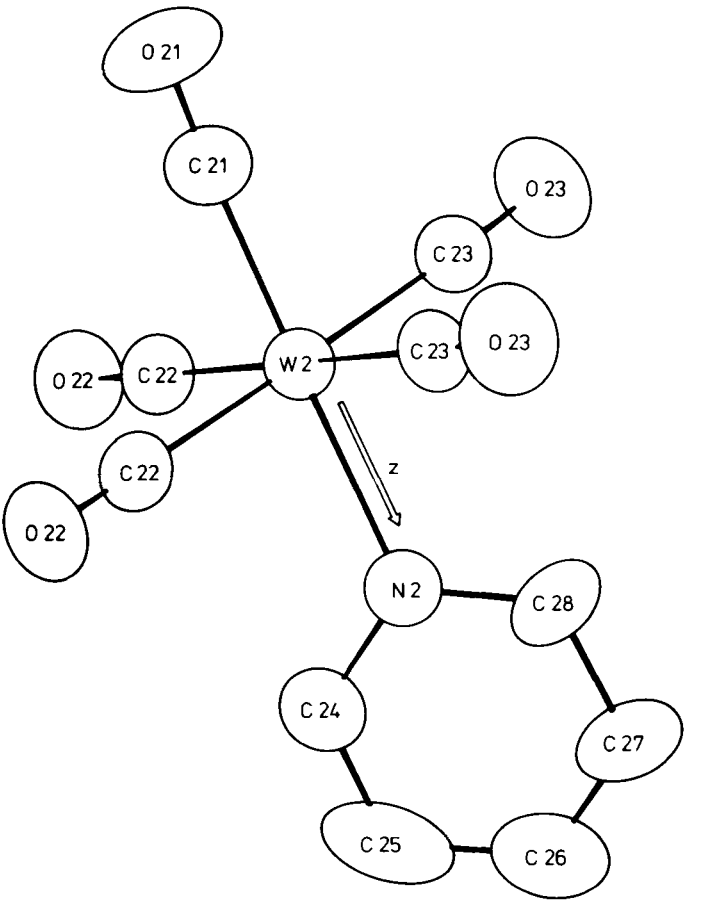

FIGURE 5 Structure of the $W(CO)_5$-pyridine complex.

consists of two alternating layers of molecules containing the molecular z axes. The crystallographic c axis is perpendicular to the z axes.[10–12]

In Fig. 6 the $\mathbf{E} \perp \mathbf{c}$ polarized emission spectra at $T = 1.9$ K, $H = 0$ T (6(a)), at $T = 7.0$ K, $H = 0$ T (6(b)), and at $T = 1.9$ K, $H = 6$ T with $\mathbf{H} \perp \mathbf{c} \perp \mathbf{O}$ (6(c)) are presented. With increasing temperature or by switching on the magnetic field, the maximum of the emission is shifted to the blue by about 300 cm^{-1}. Figure 7 shows the high-energy section of the spectra at $T = 1.9$ K, $H =$

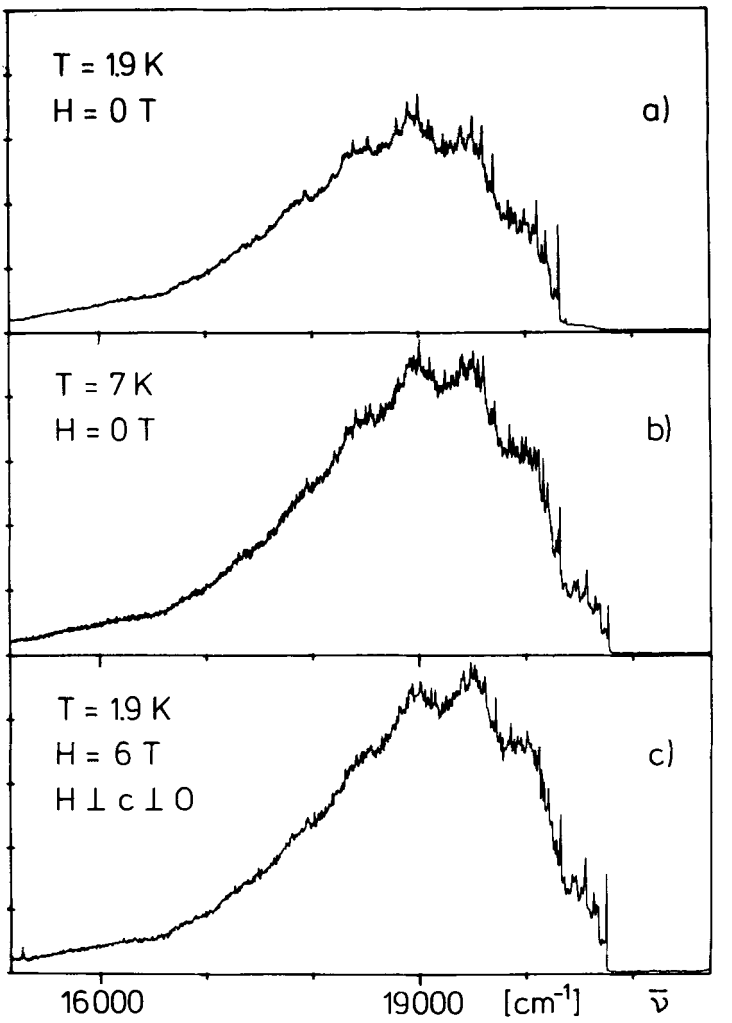

FIGURE 6 $\mathbf{E} \perp \mathbf{c}$ emission spectrum of single crystal $W(CO)_5$-pyridine. (a) $T = 1.9$ K. $H = 0$ T; (b) $T = 7.0$ K, $H = 0$ T; (c) $T = 1.9$ K, $H = 6$ T. $\lambda_{ex} = 364$ nm.

0 T (7(a)), at $T = 7.0$ K, $H = 0$ T (7(b)), at $T = 1.9$ K, $H = 6$ T (7(c)), and at $T = 7.0$ K, $H = 4$ T (7(d)) with vector orientations as in Fig. 6. By increasing the temperature and by application of the homogeneous magnetic field, an additional emission with distinct vibrational fine structure appears on the high-energy side of

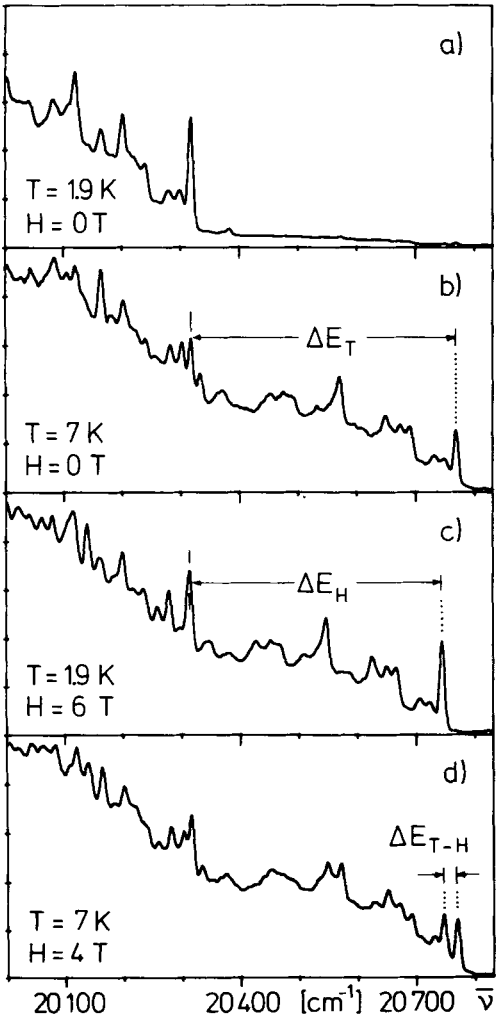

FIGURE 7 High-energy section of the E⊥c emission spectrum of single crystal $W(CO)_5$-pyridine. (a) T = 1.9 K, H = 0 T; (b) T = 7.0 K, H = 0 T; (c) T = 1.9 K, H = 6 T; (d) T = 7.0 K, H = 4 T. λ_{ex} = 364 nm.

the (7(a)) emission. A comparison of the line patterns of the temperature-induced (7(b)) and the magnetic-field-induced (7(c)) additional emission with the line pattern of the low-temperature emission at zero-field (7(a)) shows that they have very similar structure. However, the "temperature" lines appear blue-shifted by $\Delta E_T = 453\ \mathrm{cm}^{-1}$, whereas the corresponding "magnetic" lines are shifted by $\Delta E_H = 431\ \mathrm{cm}^{-1}$. The energy difference of $\Delta E_{T-H} = 22\ \mathrm{cm}^{-1}$ is demonstrated in Fig. 7(d). At $T = 7.0$ K and $H = 4$ T both effects are evidently operating and, therefore, a superposition of the "temperature" lines and the "magnetic" lines results. The intensity of the "magnetic" lines is proportional to the square of the magnetic field strength. With the vector orientation $\mathbf{H} \| \mathbf{c}$ no change of the crystal luminescence has been observed.

In the zero-field case the site of each $W(d^6)$ ion has approximately C_{4v} symmetry. The ground-state electronic configuration $b_2^2e^4$ yields the term $^1A_{1g}$, and the excited configuration $b_2^2e^3a_1^1$ the terms ^1E and ^3E. Under spin-orbit coupling (double group C_{4v}'), the low-lying ^3E splits into five progeny states $2A_1'$, A_2', B_1', B_2' and E'. The experimental results described above can be explained if $2A_1'$ and A_2' are the energetically lowest excited states as shown on the left-hand side of Fig. 8. A group-theoretical analysis predicts for the $\mathbf{E} \perp \mathbf{c}$ polarization an electrical-dipole-allowed transition between the ground state $1A_1'$ and the excited state $2A_1'$ and a (weak) vibronic transition $A_2' \rightarrow 1A_1' + a_2(\mathrm{vib})$. A comparison with Fig. 4 shows that $|0\rangle$ corresponds to $1A_1'$, $|1\rangle$ to A_2', and $|2\rangle$ to $2A_1'$.

By application of a homogeneous magnetic field $\mathbf{H} \| \mathbf{z}$ the site symmetry of each W ion is reduced from C_{4v}' to C_4', c.f., right-hand side of Fig. 8. Within this reduced symmetry the transitions between the ground state A′ and the two excited states A′ are electrical-dipole-allowed with $\mathbf{E} \perp \mathbf{c}$ polarization.

At low temperature ($T = 1.9$ K) and $H = 0$ the emission belongs to the vibronic transition $A_2' \rightarrow 1A_1' + a_2(\mathrm{vib})$ (Figs. 6(a) and 7(a)). The fine structure is due to totally symmetric vibrations. With increasing temperature, thermal repopulation of the $2A_1'$ term from the A_2' term occurs and, thus, the electrical-dipole-allowed transition $2A_1' \rightarrow 1A_1'$ becomes more and more effective. The energy difference between this transition and the $T = 1.9$ K transition equals the energy separation of the corresponding fine structure

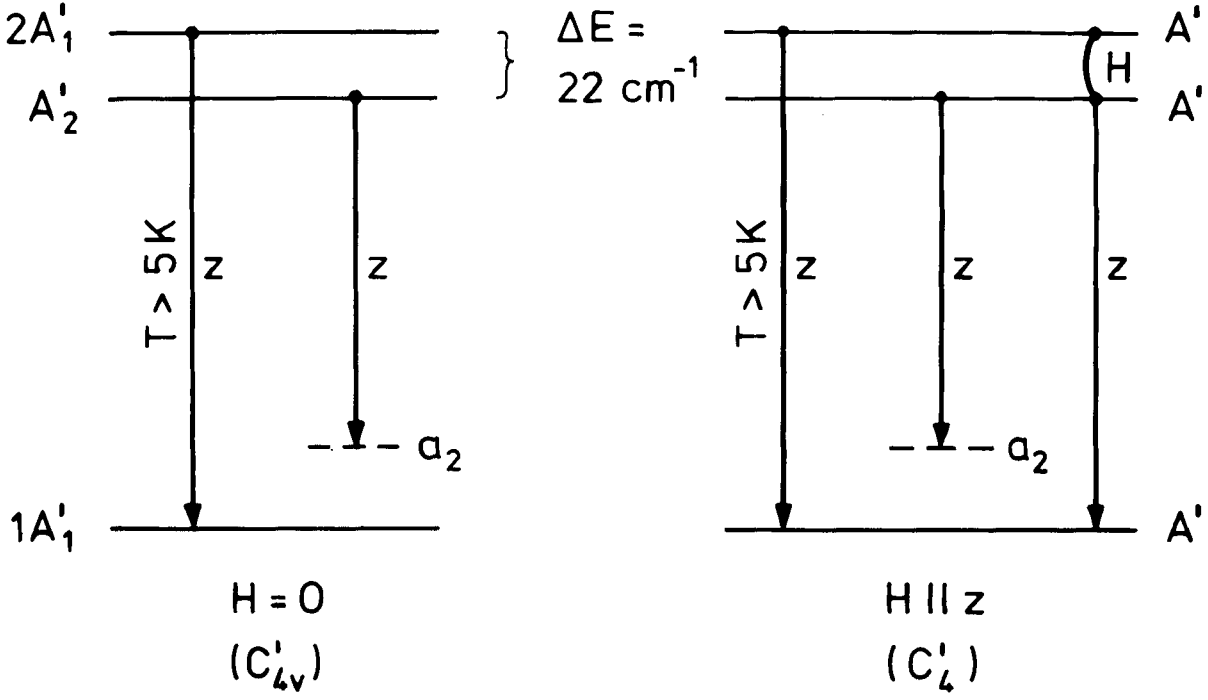

FIGURE 8 Proposed energy level diagrams of the lowest states of $W(CO)_5$-pyridine and the $\mathbf{E} \| \mathbf{z}$ polarized transitions. Left-hand side: without magnetic field (symmetry C'_{4v}). Right-hand side: under the influence of a magnetic field $\mathbf{H} \| \mathbf{z}$ (symmetry C'_4).

lines in the spectra 7(a) and 7(b): $\Delta E_T = 453\ \text{cm}^{-1} = \bar{\nu}(a_2) + [\bar{\nu}(2A_1') - \bar{\nu}(A_2')]$. The overall emission at $T > 5$ K is a superposition of both spectra, c.f., Fig. 6(b). Therefore, with increasing temperature a blue-shift of this spectrum is observed.

By application of a magnetic field $\mathbf{H} \perp \mathbf{c}$ a new radiative channel $A'(A_2') \rightarrow A'(1A_1')$ is opened, c.f., Fig. 7(c). Compared with the low-temperature zero-field spectrum, the energy difference between corresponding fine structure lines is equal to one quantum of the a_2 vibration, $\Delta E_H = 431\ \text{cm}^{-1} = \bar{\nu}(a_2)$. Since the overall emission is a superposition of both transitions, with increasing magnetic field strength a blue-shift is observed as shown in Fig. 6(c). The observed field dependence of the magnetic-field-induced emission intensity, $I_H \sim H^2$, is in agreement with the theoretical

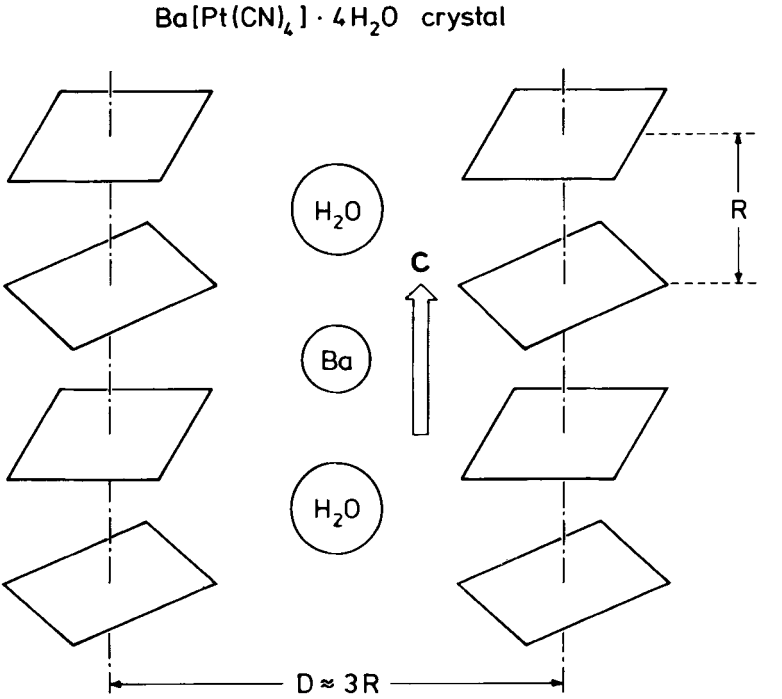

FIGURE 9 Columnar structure of the $Ba[Pt(CN)_4] \cdot 4H_2O$ crystal (schematic). Neighboring $Pt(CN)_4^{2-}$ complex ions within a chain are mutually rotated by 45° around the *c* axis.

results. At $T > 5$ K and $H > 0$ T all three transitions mentioned above will occur, c.f., Fig. 7(d). From the separation of the high-energy doublet lines the energy of the spin-orbit splitting $\Delta E_{T-H} = 22\ \text{cm}^{-1} = E(2A_1') - E(A_2')$ can be determined with high accuracy.

Tetracyanoplatinates(II)

The tetracyanoplatinates $M_x[Pt(CN)_4] \cdot nH_2O$ form crystals with quasi-one-dimensional structures as shown schematically in Fig. 9.[13] The axes of the columns formed by stacking the $[Pt(CN)_4]^{2-}$ ions are parallel to the crystallographic c-axis. The intracolumnar distance R of two neighboring complex ions is small compared to the distance between two adjacent columns and depends on the cation M and the number of crystal water molecules n. The $[Pt(CN)_4]^{2-}$ ions have D_{4h} symmetry.

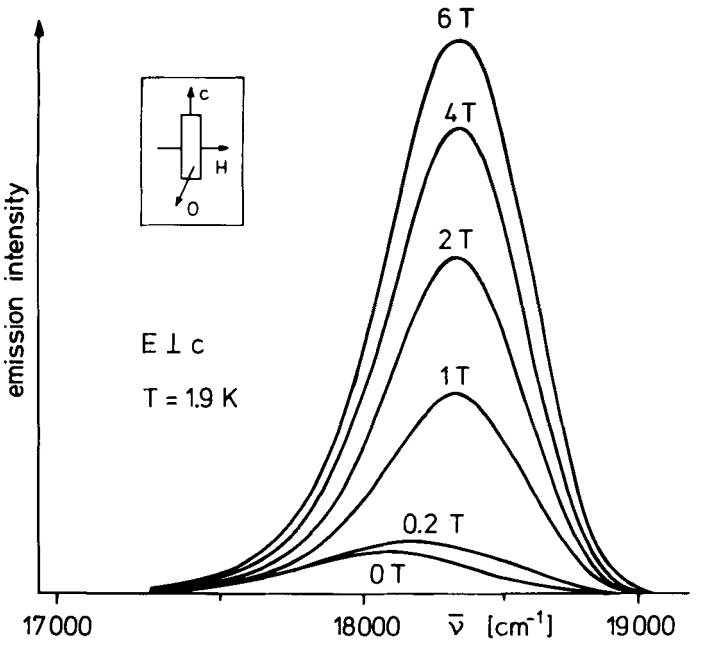

FIGURE 10 E⊥c polarized emission of single crystal $Ba[Pt(CN)_4] \cdot 4H_2O$ at several magnetic field strengths. $\lambda_{ex} = 364$ nm.

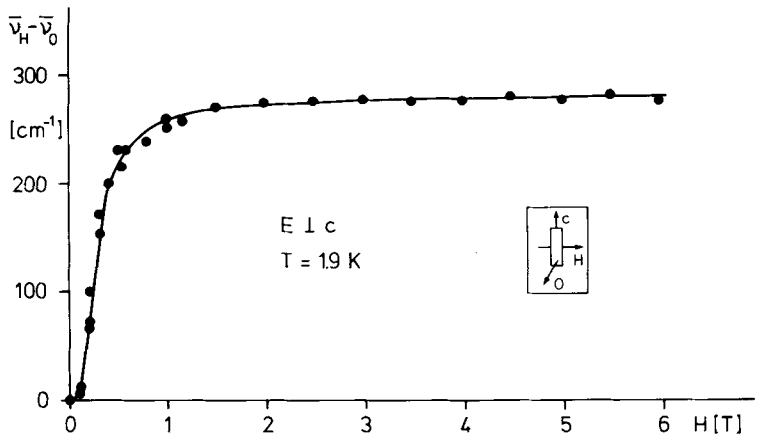

FIGURE 11 Blue-shift of the **E⊥c** polarized emission maximum of single-crystal $Ba[Pt(CN)_4] \cdot 4H_2O$ as a function of magnetic field strength. $\bar{\nu}_H$ and $\bar{\nu}_0$ are the wave numbers of the emission maximum at magnetic field strengths H and $H = 0$, respectively. $\lambda_{ex} = 364$ nm.

The **E⊥c** emission spectra of barium tetracyanoplatinate at $T = 1.9$ K for different magnetic field strengths with **H⊥c**, **H⊥O** are shown in Fig. 10.[5] With increasing magnetic field strength between 0 and 6 T, a blue-shift of the emission maximum by ~270 cm^{-1} (Fig. 11), a strong increase of the intensity by a factor of

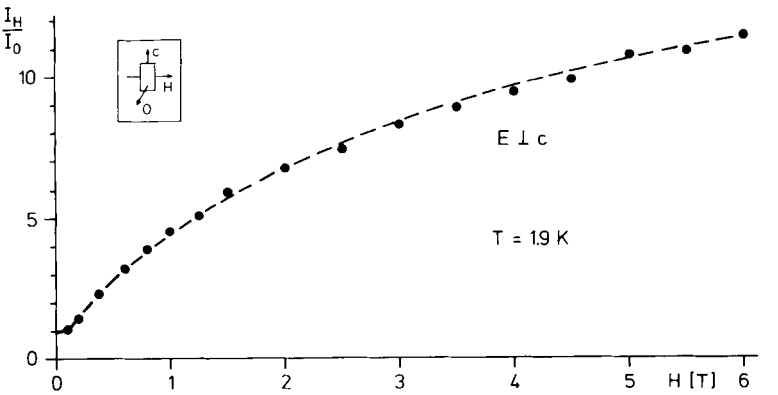

FIGURE 12 Relative intensity increase of the **E⊥c** emission of single-crystal $Ba[Pt(CN)_4] \cdot 4H_2O$ as a function of magnetic field strength. I_H and I_0 are the emission intensities at magnetic field strengths H and $H = 0$, respectively, $\lambda_{ex} = 364$ nm.

~10 (Fig. 12), and a drastic reduction of the lifetime of the emission (Fig. 13) are observed. The magnetic-field-induced change of the deactivation rate of the emitting level is a purely quadratic function of H. The rate changes over a range of more than three orders of magnitude. A similar blue-shift of the emission is observed when the temperature is raised from 1.9 K to ~20 K.

An isolated $[Pt(CN)_4]^{2-}$ ion has the ground state $^1A_{1g}(5d^8)$. The lowest excited states $^3A_{2u}$ and $^1A_{2u}$ are both obtained by raising a $5d_{z^2}$ electron to a $6p_z/\pi^*_{CN}$ orbital. In the columnar crystal packing, the complex ions interact and the excited states $^1A_{2u}$ and $^3A_{2u}$ will split into bands whose widths and energy separation depend on R.

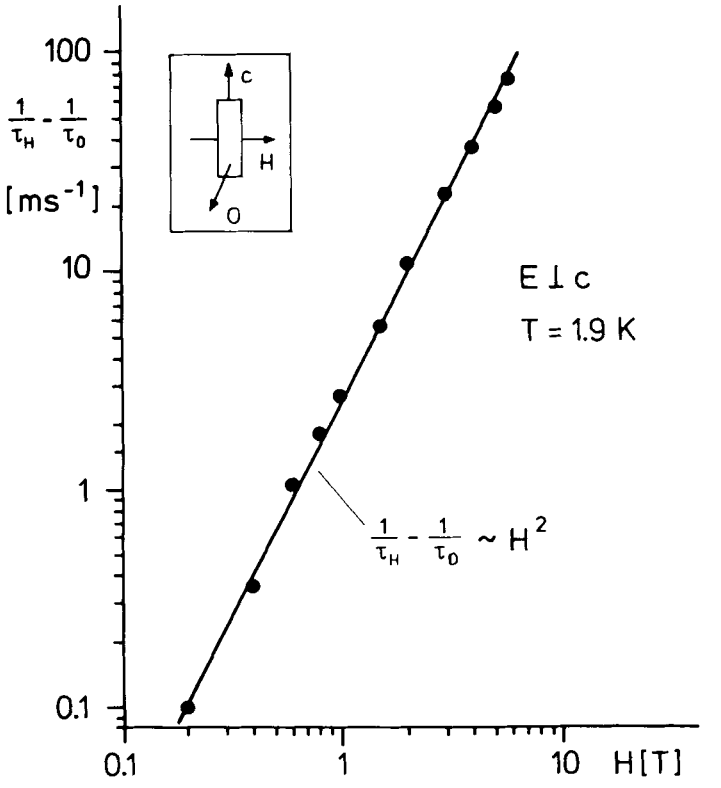

FIGURE 13 E⊥c deactivation rate of single-crystal $Ba[Pt(CN)_4] \cdot 4H_2O$ as a function of magnetic field strength. τ_H and τ_0 are the emission life times at magnetic field strengths H and $H = 0$, respectively. $\lambda_{ex} = 364$ nm.

The optical emission originates from states $^1A_{2u}$ and $^3A_{2u}$ beneath the lower edges of the corresponding bands, probably stabilized by a self-trap mechanism. By spin-orbit coupling (double group D'_{4h}) the excited triplet splits into A'_{1u} and E'_u. The experimental results described above can be explained if the A'_{1u} state is the lowest excited state, as shown in Fig. 14. A group theoretical analysis predicts an electric-dipole-allowed transition between the ground state A'_{1g} and the excited state E'_u with polarization $\mathbf{E}\perp\mathbf{c}$. The transition between A'_{1u} and A'_{1g} is symmetry forbidden. Due to vibronic coupling, however, a weak $\mathbf{E}\perp\mathbf{c}$ transition $A'_{1u} \rightarrow A'_{1g} + e_g(\text{vib})$ is expected. (A'_{1g} corresponds to $|0\rangle$, A'_{1u} to $|1\rangle$, and E'_u to $|2\rangle$ in Fig 4.)

At low temperature ($T = 1.9$ K) and with $H = 0$, the $\mathbf{E}\perp\mathbf{c}$ emission is due to the vibronic transition $A'_{1u} \rightarrow A'_{1g} + e_g(\text{vib})$. Increasing the temperature increases the thermal repopulation of the E'_u state. The transition $E'_u \rightarrow A'_{1g}$ therefore increases in intensity. The energy of this transition is larger by $\bar{\nu}(e_g) + [\bar{\nu}(E'_u) - \bar{\nu}(A'_{1u})]$ than that of the low-temperature transition. As a consequence, the overall emission, which is a superposition of both transitions, becomes blue-shifted with increasing temperature.

When a magnetic field is applied in a direction perpendicular to the fourfold symmetry axis ($\mathbf{H}\perp\mathbf{c}$), the symmetry is lowered from D'_{4h} to C'_{2h} and three energetically different levels A'_u (E'_u), $B'_u(E'_u)$, $A'_u(A'_{1u})$ of triplet parentage result, c.f., the right-hand side of Fig. 14. An important consequence of the symmetry lowering is the magnetic-field-induced mixing of the A'_u states of E'_u and A'_{1u} parentage. As a result of this mixing, in addition to the transition $A'_u(A'_{1u}) \rightarrow A'_g(A'_{1g}) + e_g(\text{vib})$, a new channel is opened leading directly to the vibronic ground state: $A'_u(A'_{1u},E'_u) \rightarrow A'_g(A'_{1g})$. The energies of the two transitions differ by the vibrational quantum $\bar{\nu}(e_g)$. In detail we expect the following three phenomena. First, with increasing magnetic field strength, the direct transition $A'_u \rightarrow A'_g$ gains intensity. This explains the large, magnetically induced blue-shift of the emission and its saturation behavior at high magnetic field strengths, when the $A'_u \rightarrow A'_g$ dominates. The saturation value of $\sim 270\ \text{cm}^{-1}$ is somewhat smaller than the molecular e_g vibration quantum of the Pt-complex ($\sim 318\ \text{cm}^{-1}$) because the emission from the E'_u cannot be totally neglected. Second, the admixture of the E'_u component

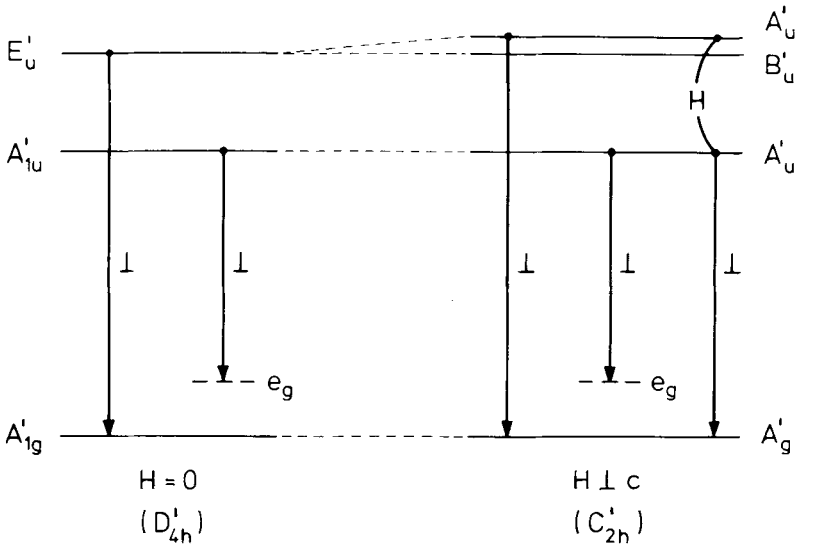

FIGURE 14 $\mathbf{E}\perp\mathbf{c}$ transitions from the lowest states of single-crystal $Ba[Pt(CN)_4] \cdot 4H_2O$ (schematic) · D'_{4h}: zero magnetic field; C'_{2h}: $\mathbf{H}\perp\mathbf{c}$.

with the A'_{1u} term explains the strong increase of intensity with increasing field strength because this component makes the transition symmetry allowed. Third, the observed H^2-dependence of the rate of radiative deactivation is due to the fact that the transition moment $\langle A'_g(A'_{1g})|\mathbf{D}|A'_u(A'_{1u}, E'_u)\rangle$ is proportional to H, as shown in the theoretical considerations.

For a magnetic field with orientation $\mathbf{H}||\mathbf{c}$, the symmetry is reduced from D'_{4h} to C'_{4h} and a new $\mathbf{E}||\mathbf{c}$ polarized channel from the A'_{1u} to the A'_{1g} is opened. Because of the relatively large energetic distance between the state A'_{1u} and the coupling excited state A'_{2u} ($^1A_{2u}$), the magnetic field effects should be much weaker than for $\mathbf{H}\perp\mathbf{c}$, in agreement with the experimental results.

Further Applications

In the last few years the method described above has been applied to several other transition metal complexes. Examples are tris(2,2'-bipyridine)ruthenium(II) sulfate[14]; numerous tetracyanoplatinates $M_x[Pt(CN)_4] \cdot nH_2O$ with M = alkali,[5] alkaline-earth,[5] rare-earth,[5,6]

and ethylenediammonium[15]; mixed crystals $Ba[Pt_{1-x}Ni_x(CN)_4] \cdot H_2O$[16]; $(Ir(2=phos)_2)ClO_4$[17]; binuclear platinum(II) complexes $Ba_2Pt_2(H_2P_2O_5)_4$[18,19] and *cis-bis*(2-phenylpyridine)platinum(II).[20]

GÜNTER GLIEMANN
Institut für Physikalische und Theoretische Chemie,
Universität Regensburg,
Federal Republic of Germany

References

1. G. L. Geoffroy and M. S. Wrighton, *Organometallic Photochemistry* (Academic, New York, 1979); G. F. Imbusch, in *Luminescence Spectroscopy*, ed. M.-D. Lumb (Academic, New York, 1978).
2. G. Gliemann, Ber. Bunsenges. Phys. Chem. **76**, 1008 (1972); P. Day, Angew. Chem. **92**, 290 (1980).
3. F. A. Cotton, *Chemical Applications of Group Theory*. Interscience (New York, 1967); H. L. Schläfer and G. Gliemann, *Basic Principles of Ligand Field Theory* (Wiley-Interscience, London, 1969).
4. H. G. Drickamer and C. W. Frank, *Electronic Transitions and the High Pressure Chemistry and Physics of Solids* (Chapman and Hill, London, 1973).
5. I. Hidvegi, W. v. Ammon and G. Gliemann, J. Chem. Phys. **76**, 4361 (1982); W. v. Ammon, I. Hidvegi and G. Gliemann, *ibid.* **80**, 2837 (1984).
6. W. v. Ammon and G. Gliemann, J. Chem. Phys. **77**, 2266 (1982).
7. C. J. Ballhausen, *Introduction to Ligand Field Theory*. (McGraw-Hill, London-New York, 1962).
8. M. Weissbluth, *Atoms and Molecules* (Academic, New York, 1978).
9. G. A. Crosby, in *Inorganic Compounds with Unusual Properties*, ed. R. B. King, Advances in Chemistry Series 150 (American Chemical Society, Washington, D.C., 1976).
10. R. Dillinger, Thesis, University of Regensburg, 1985.
11. R. Dillinger and G. Gliemann, Chem. Phys. Lett. **122**, 66 (1985).
12. J. I. Zink, private communication.
13. G. Gliemann and H. Yersin, Structure and Bonding, **62**, 87 (1985).
14. D. C. Baker and G. A. Crosby, Chem. Phys. **4**, 428 (1974).
15. R. Dillinger, G. Gliemann, H. P. Pfleger and K. Krogmann, Inorg. Chem. **22**, 1366 (1983).
16. R. Schultheiss, I. Hidvegi and G. Gliemann, J. Chem. Phys. **79**, 4167 (1983).
17. T. J. Johnson, S. D. Phillips and G. A. Crosby, Chem. Phys. Lett. **114**, 388 (1985).
18. L. Bär and G. Gliemann, Chem. Phys. Lett. **108**, 14 (1984).
19. G. A. Reisch, W. A. Turner, M. R. Corson and J. K. Nagle, Chem. Phys. Lett. **117**, 561 (1985).
20. L. Bär, G. Gliemann, L. Chassot and A. v. Zelewsky, Chem. Phys. Lett. **123**, 264 (1986).